Journal Pre-proof

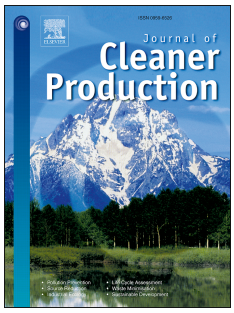

Degradation of α-nitroso-β-naphthol by UVA-B activated peroxide, persulfate and monopersulfate oxidants in water

Chao Lu, Jun Yao, Tatjana Šolević Knudsen, Meseret Amde, Jihai Gu, Jianli Liu, Hao Li, Junyang Zhang

PII: S0959-6526(19)32812-4

DOI: https://doi.org/10.1016/j.jclepro.2019.117942

Reference: JCLP 117942

To appear in: *Journal of Cleaner Production*

Received Date: 24 February 2019

Revised Date: 3 August 2019

Accepted Date: 5 August 2019

Please cite this article as: Lu C, Yao J, Knudsen TatjanaŠć, Amde M, Gu J, Liu J, Li H, Zhang J, Degradation of α-nitroso-β-naphthol by UVA-B activated peroxide, persulfate and monopersulfate oxidants in water, *Journal of Cleaner Production* (2019), doi: https://doi.org/10.1016/j.jclepro.2019.117942.

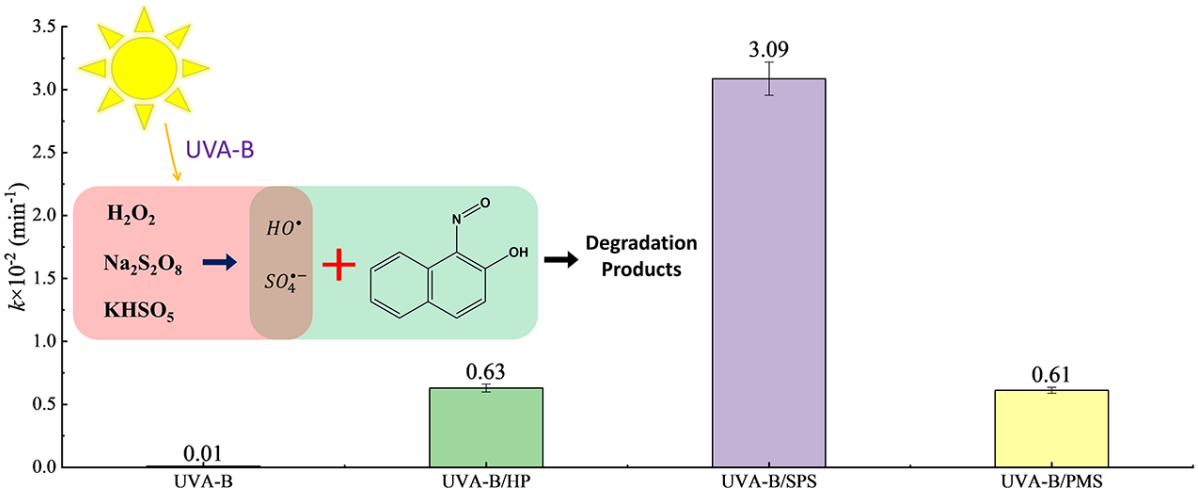

Degradation of α-nitroso-β-naphthol by UVA-B activated peroxide, persulfate and monopersulfate oxidants in water

Chao Lu[1], Jun Yao[1*], Tatjana Šolević Knudsen[2], Meseret Amde[1,3], Jihai Gu[1], Jianli Liu[1], Hao Li[1], Junyang Zhang[4]

[1]School of Water Resource and Environment, Research Center of Environmental Sciences and Engineering, China University of Geosciences (Beijing), 29 Xueyuan Road, Haidian District, 100083 Beijing, China

[2]Institute of Chemistry, Technology and Metallurgy, University of Belgrade, Njegoseva 12, 11000 Belgrade, Serbia

[3]Department of Chemistry, College of Natural and Computational Sciences, Haramaya University, P.O. Box, 138, Dire Dawa, Ethiopia

[4]Department of Mining and Metallurgical Engineering, Western Australia School of Mines, Curtin University, Kalgoorlie, WA, Australia

*Corresponding author:

E-mail: yaojun@cugb.edu.cn

Phone: +86-10-82321958

Fax: +86-10-82321958

Abstract

Flotation reagents, especially new chelating agents represented by α-nitroso-β-naphthol, are the main components of cobalt mining drainage. This study reports the degradation of α-nitroso-β-naphthol by simulated UVA-B (280–400 nm) activated systems using three common oxidants, hydrogen peroxide, sodium persulfate and potassium monopersulfate at a laboratory scale using a photoreactor. Parameters which can affect the degradation process were investigated and comparison of the degradation performance of the three systems were made. Based on the results, UVA-B/sodium persulfate system exhibited best performance towards the removal of α-nitroso-β-naphthol with a lower cost of oxidant and energy consumption compared to the others. The removal efficiency was found to increase as the oxidant dosage and the UVA-B power increases. Only potassium monopersulfate could be activated by bicarbonate and chloride ions, and SO_4^{2-} has insignificant effect on the removal efficiency of α-nitroso-β-naphthol for all systems while NO_3^- inhibited the degradation of α-nitroso-β-naphthol. In the UVA-B/hydrogen peroxide system, the hydroxyl radical had a leading role in the degradation of α-nitroso-β-naphthol, while in the other two systems, the degradation of α-nitroso-β-naphthol was mainly caused by the hydroxyl and sulphate radicals. Ten major intermediates from α-nitroso-β-naphthol degradation in the three oxidation systems were identified by gas chromatography and mass spectrometry. In summary, this report could be a great input in developing UVA-B activated oxidants-based treatment technologies. The

UVA-B/sodium persulfate system is strongly recommended for its consideration in the treatment of mine impacted wastewaters.

Capsule

UVA-B/SPS is the most efficient, economical and energy-saving technique for the degradation of αNβN compared to UVA-B/HP and UVA-B/PMS systems.

Keywords: α-nitroso-β-naphthol; UVA-B activated oxidant; Advanced oxidation processes; Kinetics; Intermediate products

1. Introduction

During the last decades, the availability of mineral rich resources which can be exploited with easy flotation is scarce, especially in China. As a result, new flotation techniques which enabled economic exploitation of low-grade sulfide ores have been emerged (Dold, 2017). As a consequence, the demand and consumption amounts of flotation reagents have been dramatically increased worldwide (Zhu et al., 2018), and more stable and highly efficient new types of flotation reagents have been emerged. α-Nitroso-β-naphthol (αNβN) (Table S1), a derivative of the simplest polycyclic aromatic hydrocarbon, naphthalene (Pozdnyakova et al., 2010), has been used as a substitute for traditional reagents. αNβN acts as a bifunctional mine chelating reagent for oxide cobaltite flotation (Hu et al., 1997) due to its active electron donating atoms, N and O (Mahmoud et al., 2010). The use of αNβN is also entertained due to its acid-resistant behavior and it is also cost effective relative to other reagents.

Despite their advantages, these reagents and their transformation products could affect the environment and the biota, and further seriously jeopardize health of human beings because of their high bioavailability (Bararunyeretse et al., 2017). They can also migrate in the environment *via* surface runoff or leaching to the groundwater, and in that way, contaminate larger water bodies. For instance, αNβN is considered to be a carcinogenic and toxic compound to the aquatic organisms (Pubchem, 2019). Besides, it is very difficult to remove such flotation reagents because of their high stability and also, since the flotation reagents cannot be recovered completely during ore

processing, some organic contaminants still existed in mine wastewaters. These indicate that an efficient and cost-effective treatment technology should be there to control such contaminations in large quantities.

Due to the deleterious-effects of persistent organic pollutants on the nature, researches on their treatment technology, particularly in mines, have attracted worldwide attention, gradually. Various physical, biological and chemical methods have been adopted to remove flotation reagents from the mine impacted wastewaters. Physical methods such as adsorption (Rezaei et al., 2018) and coagulate sedimentation (Wei et al., 2018) have certain limitations, such as high cost requirement and the collected pollutants also need re-treatment by other methods. Biological methods which include biofilters, activated sludge, and bioremediation (Cheng et al., 2012) have a long treatment cycle and the microorganisms used for the waste treatment are selective. Chemical methods like ozonation (Yan et al., 2016), photochemical (Guo et al., 2017) and metal activated oxidation processes (Chen et al., 2018) have been mainly applied in treatment of chemically stable organic pollutants. However, these methods require large quantities of chemicals and are not economical, subjected to high operation and maintenance costs. In order to develop clean, efficient and energy-saving chemical methods in the treatment of organic pollutants in mine wastewater, photolysis combined with other oxidation processes such as photoelectrooxidation (Molina et al., 2013), ozonation combined with ultraviolet radiation (Fu et al., 2015) have drawn researchers' attention.

In UV/oxidant-based advanced oxidation processes (AOPs), UVC (λ = 200–280 nm) activate the available oxidants (such as hydrogen peroxide (HP), sodium persulfate (SPS) and potassium monopersulfate (PMS)) to generate radicals such as hydroxyl radical ($HO^{\bullet}$), sulphate radical ($SO_4^{\bullet-}$) among others with its high energy radiation and demonstrated very good applicability and efficiency in practical use such as pollution control of antibiotics (Yao et al., 2013), pesticide residue (Khan et al., 2014) and other chemical syntheses (Zhang et al., 2019). However, its applicability is not economical due to the high cost and high energy consumption of UVC lamps compared with UVA-B (λ = 280–400 nm, sunlight in the UV region of the surface) (Beck et al., 2017). The use of UVA-B could be appreciated from the economical points of view, and it has been used in the photolytic degradation of organophosphorus pesticides (Weber et al., 2009) and pharmaceutical wastewater (Armaković et al., 2018).

The present work was proposed to investigate and compare the degradation of αNβN in UVA-B/ (HP, SPS and PMS) systems. In this report, UV-visible spectrophotometric method was employed for the quantitative analysis of αNβN and effects of various experimental conditions including pH, oxidant concentration, UV power and presence of anions on the αNβN degradation performance was studied, systematically. The extent of each the free radicals' contribution to the degradation process has also been assessed and the degradation products were assayed with GC-MS. It is worth mentioning that, to the best of the authors knowledge, this is the

first report to analyze and compare the αNβN degradation in the three systems. It should be also known that this work is the first of its kind to study the performance of UVA-B in activation of different oxidants, and there is no report which has compared the effects of anion concentrations on the degradation of environmental pollutants by different UVA-B activated oxidants.

2. Experimental

2.1. Chemicals and Reagents

All chemicals and reagents used in this study were of analytical grade and were used as received without any further purification. αNβN (purity, ≥ 99 %) was obtained from Thermo Fisher Scientific Inc. (Heysham, England). Selected physical and chemical properties of αNβN is provided in the Supporting Information (Table S1). A chromatographic grade methanol (Me), *tert*-butanol (TBA) and acetonitrile (ACN) were obtained from Thermo Fisher Scientific Inc. (Fair Lawn, USA). HP (H_2O_2, 30 %), SPS ($Na_2S_2O_8$, purity, ≥ 99 %), PMS ($KHSO_5 \cdot 0.5KHSO_4 \cdot 0.5K_2SO_4$, content ≥ 47 %), $NaNO_3$ (purity, ≥ 99 %), Na_2SO_4 (purity ≥ 99 %), NaCl (purity, ≥ 99 %), $NaHCO_3 \cdot 10H_2O$ (purity, ≥ 99 %), $NaH_2PO_4 \cdot 2H_2O$ (purity, ≥ 99 %), $Na_2HPO_4 \cdot 12H_2O$ (purity, ≥ 99 %), H_2SO_4 (purity, ≥ 98 %) and NaOH (purity, ≥ 96 %) were acquired from Beijing Chemical Reagents Company (Beijing, China). Ultrapure water (18.2 MΩ cm) prepared by a Direct-Q3 UV Milli-Q Water purification system (Merck

Millipore, Shanghai, China) was used throughout the experiments. Due to the low solubility of αNβN in water, its stock solution was prepared in a mixture of water and 5 % acetonitrile, and then stored at 4 ºC in dark. The solution pH was adjusted with H_2SO_4 and NaOH solutions and the pH was recorded by a PE28-Standard pH meter (METTLER TOLEDO, Shanghai, China). The initial pH was adjusted before addition of oxidant, anions and free radical scavenger.

2.2. Photolysis of αNβN using UVA-B Radiation

Photolysis experiments were carried out with a photoreactor BL-GH-V instrument (Bilon, Shanghai, China). The photolysis has been done at various pH, UVA-B radiation power, as well as at various concentrations of the oxidants and anions. The predominant radicals were identified using TBA as $HO^{\bullet}$-scavenger and Me as $HO^{\bullet}$ and $SO_4^{\bullet-}$-scavenger. In detail, 50 mL of 0.1 mM αNβN solution was transferred into a cylindrical quartz tube with a fixed stirring speed (500 rpm), and the oxidizing reagent was added thereto. After adjusting the UVA-B power, the reaction was conducted in an optical reactor, by irradiating UVA-B radiation using an UV mercury lamp equipped with a filter that provide a light source from 280 to 400 nm. The instrument was equipped with a condenser and the temperature in the water circulation device was controlled at 25±1 °C. When the reaction proceeds to 0, 10, 20, 30, 60, 90, 120 min, the experimental samples (1.5 mL) were taken out at predetermined time intervals and the reaction was quenched, immediately, with Me. After being placed in

the Vortex-5 vortex mixer (Kylin-bell, Jiangsu, China) for 1 min, the solution was filtered through organic nylon membrane (pore size, 0.22 μm) prior to analysis with a DR6000 UV-vis spectrophotometer (HACH, Beijing, China) equipped with a 1 cm rectangular miniature colorimetric dish (capacity, 1.5 mL) at a wavelength of 378 nm. All irradiation experiments and absorbance measurements were conducted in triplicates.

2.3. UV-vis and GC-MS Analysis

In this study, the concentration of αNβN was determined, quantitatively, with the UV-Vis spectrophotometer (see Text S1 in Supplementary Information for reliability of the method). An external calibration curve was plotted (refer Fig. 2 Inset in Text S1) and used to calculate the analyte concentrations and the analysis results were expressed as an average with a standard deviation (n = 3).

Using the concentration of αNβN measured at specific time intervals during the experiment, the percentage of αNβN removal, Y (%), was calculated according to Eq. (1).

For all kinetic experiments performed under different conditions, the degradation of αNβN was fitted with the pseudo-first-order kinetic equation (Eq. (2)) and the corresponding value were obtained from the slope obtained by plotting $\ln(C_0/C_t)$ versus t.

$$Y(\%) = \frac{C_0 - C_t}{C_0} \times 100\ \% \quad (1)$$

$$ln(C_t/C_0) = -kt \quad (2)$$

Where, C_0 (mM) and C_t (mM) are the αNβN concentrations at the initial and *t*-times (min); *k* (min^{-1}) is the degradation kinetic constant of the quasi first order kinetics.

An Agilent 7890B gas chromatograph (GC) equipped with an Agilent 5977B mass selective detector (MS) (Agilent Technologies, Santa Clara, CA, USA) was employed to identify the αNβN degradation intermediate products. Separation of the analytes was achieved using HP-5MS (5 % phenyl methylsiloxane) capillary column (30 m × 0.25 mm, 0.25 μm). Liquid-liquid extraction was made by addition of ethyl acetate to the sample at 1:2 ratio (*v/v*) and the mixture was vortexed. The mixture was left undisturbed for a few minutes until the layers have completely separated. Thereafter, an appropriate amount of the upper (organic) layer was transferred to a gas phase vial and analyzed by GC-MS. The solution was injected (injection volume, 1 μL) in splitless mode while the inlet temperature was 280 °C. The column temperature program was as follows: the initial temperature 50 °C was held for 2 minutes and raised to 150 °C at 10 °C/min, then raised to 200 °C at 5 °C/min, and finally increased to 290 °C at 10 °C/min. The entire process took 31 minutes for a single injection. Mass spectra, recorded from m/z 50–500, were obtained in an electron impact ionization mode (EI^+) at 70 eV and the temperature of ion source and quadrupole was 230 °C and 150 °C. The data were analyzed using a mass spectral search program

(NIST 14, USA) and the spectra were compared with those of the standards in the NIST library.

2.4. Economical Aspect of the Processes

To investigate the economical aspect of the current methods, E_{EO} (Electrical energy per order, kWh m^{-3} $order^{-1}$) which is the electrical energy in kWh required to degrade a contaminant C by one order of magnitude in 1 m^3 of contaminated water was calculated, and the calculation was made according to the following expressions (Bolton, et al., 2001):

$$E_{ED} = \frac{Pt}{60V} \quad (3)$$

$$E_{EO} = \frac{E_{ED}}{\log(C_i/C_f)} \quad (4)$$

Where, P is the UVA-B lamp power (W), t is the illumination time (min), V is the total treatment solution volume (L), C_i and C_f represent the initial and final αNβN concentrations (mM).

3. Results and Discussion

3.1. UVA-B based Photolysis of αNβN

As can be seen from Fig. 1(a), there is a negligible removal of αNβN using UVA-B radiation without oxidant over a period of 120 min which indicate that

UVA-B irradiation alone is not enough to degrade the αNβN. This might be due to the fact that organic molecules absorb photons at the specified wavelength(s) to produce an electronically excited state molecules, and chemical decomposition of the excited state molecule is competitive with a physical deactivation process to non-excited state molecule (Eq. (5)) (Parsons, 2004). In this experiment, decomposition of excited αNβN molecules may be in an inferior position in the competition, or αNβN molecules does not reach the excited state, because UVA-B radiation may not provide sufficient energy for the αNβN decomposition. It can be concluded that the UVA-B alone cannot degrade αNβN effectively.

In addition to this, the degradation profile of αNβN with the oxidants in the absence of UVA-B radiation was investigated. As can be seen from the results (Fig. 1(b)), the pseudo-first-order kinetic constants (*k* values) of αNβN removal was found to be 0.0001 min^{-1} by HP, 0.0003 min^{-1} by SPS and 0.0005 min^{-1} by PMS. These show that αNβN was feebly degraded in the presence of PMS oxidant while HP and SPS are incapable to remove the αNβN, significantly.

$$R \xrightarrow{hv} R^{*} \rightarrow R/By\text{-}Products \qquad (5)$$

Where R represent non-excited state molecule and R^{*} represent excited state molecules.

Oxidant is the main source of free radicals in the AOPs system. Before evaluating the effects of experimental parameters on degradation process, comparison of the removal efficiency of αNβN was made in the UVA-B/oxidation systems without pH

adjustment.

In contrast to the absence of UVA-B radiation (Fig. 1(b)), UVA-B/oxidant systems showed a high αNβN degradation efficiency which might be attributed to the O-O bond homolytic fission from H_2O_2, $S_2O_8^{2-}$ and HSO_5^- molecules under UVA-B radiation (reactions 1–3 in Table S2). In this process, the oxidants, HP (E^0=1.80 V) (Neyens and Baeyens, 2003), SPS (E^0=2.01 V) (Ghanbari et al., 2016) and PMS (E^0=1.82 V) (Ghanbari et al., 2016) can generate $HO^{\bullet}/H_2O$ (E^0=1.80–2.70 V) (Buxton et al., 1988) or $SO_4^{\bullet-}/SO_4^{2-}$ (E^0=2.50–3.10 V) (Sharma et al., 2015) radicals, which accounts for the αNβN degradation.

In the UVA-B/oxidant systems without adjusting the initial pH, the removal efficiency of αNβN followed a decreasing order of UVA-B/SPS >> UVA-B/HP ≈ UVA-B/PMS with the corresponding pseudo-first-order kinetic constants of 0.0309, 0.0063 and 0.0061 min^{-1}, (Fig. 1). Such differences might be due to the differences in the molecular structure and properties of HP, SPS and PMS (Ao and Liu, 2017) and it should be also noted that the activation effect of SPS is much higher than that of HP and PMS. The reasons for such observation may be as follows: On one side, the O-O bond of $S_2O_8^{2-}$ has a longer bond length and lower bond energy than H_2O_2 and SO_5^-, indicating that SPS decompose, easily, than the others under UVA-B irradiation (Yang et al., 2010) and the apparent quantum yield of $SO_4^{\bullet-}$ (Φ=1.4 mol E s^{-1} (deoxidation) or Φ=1.8 mol E s^{-1} (oxygen saturation)) (Mark et al., 1990) in the UVA-B/SPS system is higher than that of $HO^{\bullet}$ (Φ=1.0 mol E s^{-1}) (Baxendale, 1957) in UVA-B/HP

system and $SO_5^{\bullet-}$ (pH=7, Φ=1.04 mol E s^{-1}) (Guan et al., 2011) in UVA-B/PMS system. On the other side, the consumption rate of $S_2O_8^{2-}$ to $SO_4^{\bullet-}$ in the UVA-B/SPS system (reaction 7 in Table S2, k = 6.1×10^5 $M^{-1}s^{-1}$) is considerably lower than that of $HO^\bullet$ (reaction 4 in Table S2, k= 2.7×10^7 $M^{-1}s^{-1}$) in the UVA-B/HP system, and the rate of reorganization of $SO_4^{\bullet-}$ (reaction 28 in Table S2, k = 3.1×10^8 $M^{-1}s^{-1}$) is almost 10 times slower than the $HO^\bullet$ (reaction 11 in Table S2, k = 4.2×10^9 $M^{-1}s^{-1}$). The lifetime of $SO_4^{\bullet-}$ (3×10^{-5} – 4×10^{-5} s) is higher than that of $HO^\bullet$ (2×10^{-8} s) (Ghanbari et al., 2016), and $SO_4^{\bullet-}$ has a higher steady-state concentration (Kwon et al., 2015).

3.2. Effects of the Experimental Conditions

Solution pH (Ao and Liu, 2017), oxidant concentration, UVA-B power and anions (Alsaiari and Tang, 2018) such as NO_3^-, SO_4^{2-}, Cl^-, and HCO_3^- were also reported to be among the predominant factors which could influence the performance of the UV-activated oxidants. Accordingly, investigation of the effects of these conditions on the degradation processes is important.

3.2.1. Effect of pH

To learn the effect of pH, the removal efficiency of αNβN at different solution pH was explored and the results (Table 1) indicate that, when SPS and PMS oxidants are added to the system, the solution pH decreases, immediately. For instance, a solution with initial pH of 9.0 or 11.8 changes to 6.2 or 6.3 after addition of SPS or PMS

(Table 1). In the UVA-B/HP system, the solution pH solution is almost unchanged when HP is added to the reaction solution which might be due to its weak acidity. When the solution pH is between 4.0 and 6.8, the pseudo-first-order kinetic constants of αNβN decay is stable between 0.0062 and 0.0064 min^{-1} and decreases to 0.0054 min^{-1} when the solution pH is lowered to 2.0. In the UVA-B/SPS or UVA-B/PMS systems, the pseudo-first-order kinetic constants of αNβN decay is stable between 0.030 or 0.0056 and 0.032 or 0.0064 min^{-1} when the solution pH is between 1.9 or 2.3 and 6.2 or 7.4). In general, UVA-B/SPS system was found to be the most efficient within the considered pH values, and impact of change in pH on αNβN removal efficiency is not significant.

3.2.2. Effect of oxidant concentration

The effect of oxidant concentration on αNβN degradation was investigated in the concentration ranges of 5–100 for HP and PMS, and 2–50 mM for SPS. Other experimental conditions were held unaffected and the results are presented in Fig. 2(a–c). For the three oxidants, the removal efficiency of αNβN was found to increase as their concentration increases (Fig. 2(a–c)). At SPS concentrations of 10 mM, maximum removal efficiency (97.8 %) of αNβN were achieved, and at HP and PMS concentrations of 50 mM, maximum removal efficiency (94.7 % and 98.2 %) of αNβN were achieved, after 120 min of irradiation time. Higher removal efficiency of αNβN in the presence of higher amount of the oxidants might be attributed to the

increased yield of $HO^{\bullet}$ and/or $SO_4^{\bullet-}$ radicals. On the other hand, Devi and his co-authors (Devi et al., 2016) reported that in the presence of excessive amounts of oxidants, the oxidants themselves may consume the free radicals (reactions 4–10 in Table S2), which in turn inhibits the oxidation process. In this study, no adverse effects associated to the oxidant concentration was observed on the αNβN degradation, possibly because the maximum oxidant concentration used might be below the oxidant threshold level.

The linear increase of first-order kinetic *k* values for the degradation of αNβN under different systems with the oxidant dosage (Fig. 2(d)) also suggests that αNβN removal is dependent on the initial oxidants concentration. From these results, it can be also concluded that SPS has better degradation performance than HP and PMS.

3.2.3. Effect of UVA-B power

The effect of UVA-B powers on αNβN degradation was investigated in the range from 200 to 600 W for the three systems keeping other conditions constant. In the three oxidation systems investigated, the removal efficiency of αNβN was found to increase as the UVA-B power increased. At SPS concentrations of 10 mM, maximum removal efficiency (99.1 %) of αNβN was achieved, and at HP and PMS concentrations of 50 mM, maximum removal efficiency (98.5 % and 99.0 %) were achieved, after 600 W UVA-B irradiation for 120 min (Fig. 3(a–c)). Similarly, from the index increase of the pseudo-first-order kinetic *k* values with an increase in the

UVA-B power (Fig. 3(d)). It can be concluded that αNβN degradation efficiency depends on the power strength which is consistent with the report of Muruganandham and Swaminathan (Muruganandham and Swaminathan, 2004). The results also suggested that UVA-B/SPS exhibit better degradation performance than the UVA-B/HP and UVA-B/PMS systems (Fig. 3(a–c)).

3.2.4. Effect of different anions

In order to explore and monitor the anions effect on UVA-B/oxidant systems, the effects of NO_3^-, SO_4^{2-}, Cl^-, and HCO_3^- were investigated, systematically, by varying the anions concentration in the range of 0.1–10 mM, keeping other conditions unaltered.

Effect of nitrate concentration. As can be seen from Fig. 4, the pseudo-first-order kinetic *k* values lowered from 0.0063 to 0.0051, 0.031 to 0.026, and 0.0061 to 0.0058 min^{-1} in UVA-B/HP, UVA-B/SPS and UVA-B/PMS system, as the amount of NO_3^- increased from 0.1 to 10 mM in all systems. This effect may be caused by photolysis of NO_3^- and subsequent formation of NO_2^- (reaction 34 in Table S2) which can absorb and block UV light transmission through aqueous solutions (Ao and Liu, 2017). Although some authors (Spiliotopoulou et al., 2015) reported that NO_3^- can produce $HO^\bullet$ (reaction 35 in Table S2) in aqueous solution under UV irradiation, which accelerates the degradation process, this can be simply ignored since it occurs, significantly, only under UVC light. Additionally, NO_3^- can react with $SO_4^{\bullet-}$ to

generate reactive groups, $NO_3^{\bullet}$ (reaction 36 in Table S2), which would compete with $HO^{\bullet}$ and $SO_4^{\bullet-}$ for the reaction with αNβN and lead to a decrease in αNβN degradation efficiency.

Effect of sulfate concentration. In this experiment, the effect of SO_4^{2-} on the UVA-B/oxidant systems was found to be insignificant (Fig. 4). The pseudo-first-order kinetic *k* values of αNβN decay were stable between 0.0058–0.0063 min^{-1} in UVA-B/HP, 0.0031–0.0035 min^{-1} in UVA-B/SPS and 0.0054–0.0061 min^{-1} in UVA-B/PMS systems. These results can be explained with the reactions provided in Table S2 (reactions 37–39 in Table S2). Accordingly, the existing SO_4^{2-} undergoes these reactions, which lead to the consumption of reactive intermediates (radicals) without generating new ones and the reactions terminate. In the case of UVA-B/SPS system, further increase in SO_4^{2-} concentration caused slight increment to the αNβN removal efficiency which might be attributed to the formation of $S_2O_8^{2-}$ from the reaction between SO_4^{2-} and $SO_4^{\bullet-}$ (reaction 39 in Table S2).

Effect of chloride concentration. Compared with the effects of NO_3^- and SO_4^{2-}, the amount of Cl^- has a significant contribution to the degradation of αNβN in the UVA-B/PMS system. As the Cl^- concentration increases from 0.1 to 10 mM, the αNβN removal efficiency also increases, pseudo-first-order kinetic *k* value increased from 0.0061 to 0.14 min^{-1} (Fig. 4(c)). This may be due to the formation of active compounds such as HOCl and Cl_2 from the Cl^- (reactions 59–60 in Table S2) (Lente et al., 2009), which enhance the αNβN degradation.

In the UVA-B/HP system, Cl^- demonstrated an inhibitory effect on the αNβN degradation which may be due to the consumption of $HO^\bullet$ by Cl^- to form $ClOH^{\bullet-}$ which can react with H^+ to form $Cl^\bullet$, which further generate $Cl_2^{\bullet-}$ and Cl_2 (E^0=1.40 V) (Babuponnusami and Muthukumar, 2014) (reactions 40–41 and 45–48 in Table S2). The output of the reaction between $HO^\bullet$ and Cl^- was reported to be pH dependent, and in basic media (pH, >7.2), the major product is $ClOH^{\bullet-}$ (reactions 55–56 in Table S2), while below 7.2 pH value, $Cl^\bullet$ and $Cl_2^{\bullet-}$ become the major free radicals (Deng et al., 2013). Since the redox potential of the $Cl^\bullet/Cl^-$ group (E^0=2.40 V) (Shah et al., 2013) is close to $HO^\bullet/H_2O$ (E^0=1.80–2.70 V), when 0.1 mM Cl^- is added, the pseudo-first-order kinetic *k* value of αNβN degradation decreases from 0.0063 to 0.0050 min^{-1}. However, as the Cl^- concentration increases, the total population of $Cl^\bullet$ and $Cl_2^{\bullet-}$ increases and the removal efficiency of αNβN tends to increase as well, even though the efficiency is still below the experimentation made without addition of Cl^- (Fig. 4(a)).

Similar to the UVA-B/HP system, Cl^- addition to the UVA-B/SPS system also negatively affects the αNβN removal since the responsible free radical, $SO_4^{\bullet-}$, might be consumed by the Cl^- to generate $Cl^\bullet$ and $Cl_2^{\bullet-}$ (reactions 43–48 in Table S2). This is logical as the redox potential of the $Cl^\bullet/Cl^-$ group (E^0=2.40 V) is lower than the $SO_4^{\bullet-}/SO_4^{2-}$ (E^0=2.50–3.10 V) (Tan et al., 2012). In the system where the Cl^- concentration varies in the range 0.1–5 mM, the pseudo-first-order kinetic *k* value was found to decrease from 0.031 to 0.021 min^{-1} (Fig. 4(b)), and start to increase as the

Cl^- dosage increased from 5 to 10 mM. This effect might be caused by the excessive reactive chlorine groups ($Cl^•$) which promote the formation of $SO_4^{•-}$ (reaction 54 in Table S2). Since the oxidative ability of $SO_4^{•-}$ for αNβN is more significant than that of $Cl^•$, $Cl_2^{•-}$ and $HO^•$, the UVA-B/SPS system require a higher amount of Cl^- than the UVA-B/HP system. Because of that, the removal efficiency of αNβN showed an increasing trend at higher Cl^- concentrations.

Effect of bicarbonate concentration. Generally, being a radical quencher, HCO_3^- was previously thought to have a negative effect on these processes (Zhou et al., 2013). This was observed in the results of the current study for the UVA-B/HP and UVA-B/SPS systems, in which the αNβN degradation pseudo-first-order kinetic *k* values were found to decrease from 0.0063 to 0.0039 min^{-1} and from 0.031 to 0.017 min^{-1}, as the amount of HCO_3^- increased from 0 to 10 mM (Fig. 4(a and b)). In acidic media (e.g. pH = 6), some amounts of the HCO_3^- reacts with the existing hydrogen ions (reaction 57 in Table S2), and the unconsumed HCO_3^- could interact with $HO^•$ and $SO_4^{•-}$ (reactions 58 and 59 in Table S2) which thwarts the degradation efficiency. An accelerated removal of αNβN observed (pseudo-first-order kinetic *k* value increases from 0.011 to 0.016 min^{-1}) when the addition of HCO_3^- varied from 5 to 10 mM in the UVA-B/PMS system (Fig. 4(c)) may be due to the fact that HSO_5^- has an asymmetric structure contrary to the H_2O_2 and $S_2O_8^{2-}$. The SO_3 group can attract electrons, and the electron cloud of the O-O bond tends to be on the SO_3 side, causing the O on the H side to be positively charged (Yang et al., 2010). PMS with this

asymmetric structure are easily attacked by nucleophiles (Betterton and Hoffmann, 1990). Since HCO_3^- has one nucleophilic atom O^- which can attack O-O bond, PMS will be activated by the HCO_3^- faster relative to HP and SPS. It has been also reported that although the redox potential of the $HCO_3^{\bullet}/HCO_3^-$ group (E^0=1.63 V) (Bennedsen et al., 2012) is lower than that of $HO^{\bullet}$ and $SO_4^{\bullet-}$, $HCO_3^{\bullet}$ has a very high selectivity for contaminants degradation compared to $HO^{\bullet}$ and $SO_4^{\bullet-}$ (Devi et al., 2016).

3.3. Reactions with radical scavenging

To identify the extent of $HO^{\bullet}$ and $SO_4^{\bullet-}$ contribution to the αNβN removal in the three oxidation systems, TBA was used as a free radical scavenger to capture $HO^{\bullet}$ (reaction 30 in Table S2) and Me as an efficient $HO^{\bullet}$ and $SO_4^{\bullet-}$-scavenger (reactions 32–33 in Table S2) (Xie et al., 2015). Accordingly, the contributions of $HO^{\bullet}$ and $SO_4^{\bullet-}$ was identified on the ground of the difference of pseudo-first-order kinetic *k* value of αNβN degradation.

As shown in Fig. 5(a), addition of TBA to the UVA-B/HP system significantly reduced the degradation efficiency of αNβN. The *k* value of αNβN decay was found to decrease from 0.0063 to 0.00086 min^{-1}. Addition of TBA to the UVA-B/SPS system and UVA-B/PMS system showed a clear removal effect (the *k* values of αNβN decay were found to decrease from 0.031 to 0.014 min^{-1} and from 0.0061 to 0.0037 min^{-1}), while the addition of Me resulted in a significant quenching effect (the pseudo-first-order kinetic *k* values of αNβN decay were found to decrease from 0.031

to 0.0054 min^{-1} and from 0.0061 to 0.0015 min^{-1}) (Fig. 5(b–c)). These results clearly indicate that the $HO^{\bullet}$ plays a leading role in the degradation of αNβN in the UVA-B/HP system, while in the other two systems, the degradation of αNβN is mainly caused by $HO^{\bullet}$ and $SO_4^{\bullet-}$ radicals. In the UVA-B/SPS system, the formation of $SO_4^{\bullet-}$ is mainly due to the photolysis of SPS, the decay of $S_2O_8^{2-}$ (reactions 13–14 in Table S2) and the process of OH^--activated SPS (reactions 15–17 in Table S2). Because of the interaction of $SO_4^{\bullet-}$ with water molecules (reaction 18 in Table S2), $HO^{\bullet}$ is also formed. In addition, excess SPS reacts with $HO^{\bullet}$ to form $SO_4^{\bullet-}$ (reaction 6 in Table S2).

In the UVA-B/PMS system, the free-radicals, $HO^{\bullet}$ and $SO_4^{\bullet-}$, are mainly generated from the photolysis of PMS. Excessive PMS will consume $HO^{\bullet}$ and $SO_4^{\bullet-}$ and generate $SO_5^{\bullet-}$ (reactions 8–10 in Table S2), and the decay of $SO_5^{\bullet-}$ (reaction 21 in Table S2) could generate $SO_4^{\bullet-}$. In addition, the process by which PMS reacts with water molecules to form HP may also accelerate the αNβN destruction (reaction 19 in Table S2).

3.4. Intermediate products identification

In order to identify the αNβN intermediates products and thereby investigate the difference of αNβN degradation in UVA-B/(HP, SPS and PMS), reaction mixtures of the three systems were analyzed by GC-MS after 0, 60, and 120 min of irradiation time. The information on the possible degradation products of αNβN in the three

UVA-B/oxidant systems extracted from the GC-MS analysis is shown in Table 3. Based on the GC-MS chromatograms (Fig. S1–Fig. S3), about 10 major intermediate products were identified and recorded (Table 3). In the three systems, when the reaction last for 120 min, αNβN was almost completely degraded, albeit some intermediate products were detected. It is worth mentioning that 1,2-benzenedicarboxaldehyde (product 2) was not detected in UVA-B/HP and UVA-B/PMS systems. Comparing the differences of the chromatogram at 0, 60, and 120 min in different systems, the results shows that, 2-cyanobenzaldehyde (product 1), 2-cyanobenzaldehyde (product 3), phthalic anhydride (product 4), 1(3H)-isobenzofuranone (product 5) and o-cyanobenztaoic acid (product 8) hardly undergo degradation in different systems. Even though other compounds were observed in the analysis, they are not well matched to the library profile for identification, and not discussed here. It should be also noted that since the GC-MS system with non-polar column which was used in this study can only detect low-polar products, the use of other instrumental techniques is recommended in future studies.

3.5. Economic Comparison

To compare the energy requirements of the current UVA-B-based AOPs in degradation of αNβN, the E_{EO} was calculated for each of the oxidation processes and the results are provided in Table 2. As can be seen from the results (Table 2), the E_{EO} values of the three oxidation systems follow a decreasing order of UVA-B/SPS >

UVA-B/HP ≈ UVA-B/PMS. Since the higher the E_{EO} value shows the higher the power utilization efficiency, SPS is cost effective relative to HP and PMS. In summary, the UVA-B/SPS process is the most efficient and economically friendly technique for the αNβN degradation. In the literature, persulfate was also reported to be efficient and economical relative to the two systems for the degradation of an azo dye and Acid Orange 7 (Yang et al., 2010), and a dye and brilliant green (Rehman et al., 2018) which are in good agreement with this report.

4. Conclusions

In this study, the use of UVA-B/(HP, SPS, and PMS) systems were studied for the degradation of αNβN in aqueous solution using UV-vis spectrophotometer and the pseudo-first-order kinetics of αNβN degradation was followed in all cases. The obtained results indicated that UVA-B alone is not enough for the αNβN degradation and the decomposition efficiency of αNβN was found to accelerate in the presence of HP, SPS and PMS oxidants. Among the three UVA-B-based AOPs systems, UVA-B/SPS is efficient from the energy consumption and economy points of view. Under acidic conditions, the effect of pH was insignificant and increase in the oxidant dosage and UV power enhanced the removal efficiency of αNβN in the systems. In addition, chloride and high concentration of bicarbonate ions were found to affect the activity of PMS, positively. In the UVA-B/HP system, $HO^{\bullet}$ plays a leading role in the degradation of αNβN, while $HO^{\bullet}$ and $SO_4^{\bullet-}$ are the main reactive species in the other

two systems. In general, the UVA-B techniques particularly the UVA-B/SPS system is more or less green, cost effective and efficient oxidation process, and its consideration in the treatment of mine impacted wastewaters is strongly recommended.

Supporting Information

The Supporting Information is available free of charge on the Internet.

Notes

The authors declare no competing interest.

Acknowledgements

This work is supported in part by grants from the National Science Foundation of China (41430106, 41720104007, 41573080, 41711530030，41711530150) and project of the Ministry of Science and Technology of China (S2016G2135). This research was also in part financed by the Ministry of Education, Science and Technological Development of the Republic of Serbia (Project No 176006) and by the International Joint scientific and technical collaboration between People's Republic of China and Republic of Serbia as a part of the Project number 4-18.

References

Alsaiari, A., Tang, H.L., 2018. Field investigations of passive and active processes for acid mine drainage treatment: Are anions a concern? Ecol. Eng. 122, 100-106.

Ao, X., Liu, W., 2017. Degradation of sulfamethoxazole by medium pressure UV and oxidants: Peroxymonosulfate, persulfate, and hydrogen peroxide. Chem. Eng. J. 313, 629-637.

Armaković, S.J., Armaković, S., Četojević-Simin, D.D., Šibul, F., Abramović, B.F., 2018. Photocatalytic degradation of 4-amino-6-chlorobenzene-1,3-disulfonamide stable hydrolysis product of hydrochlorothiazide: Detection of intermediates and their toxicity. Environ. Pollut. 233, 916-924.

Babuponnusami, A., Muthukumar, K., 2014. A review on Fenton and improvements to the Fenton process for wastewater treatment. J. Environ. Chem. Eng. 2(1), 557-572.

Bararunyeretse, P., Yao, J., Dai, Y., Bigawa, S., Guo, Z., Zhu, M., 2017. Toxic effect of two kinds of mineral collectors on soil microbial richness and activity: analysis by microcalorimetry, microbial count, and enzyme activity assay. Environ. Sci. Pollut. Res. Int. 24(2), 1565-1577.

Baxendale, J.H., Wilson, J.A., 1957. The photolysis of hydrogen peroxide at high light intensities. Trans. Faraday Soc. 53, 344-356.

Beck, S.E., Ryu, H., Boczek, L.A., Cashdollar, J.L., Jeanis, K.M., Rosenblum, J.S., Lawal, O.R., Linden, K.G., 2017. Evaluating UV-C LED disinfection performance and investigating potential dual-wavelength synergy. Water Res. 109, 207-216.

Bennedsen, L.R., Muff, J., Søgaard, E.G., 2012. Influence of chloride and carbonates on the reactivity of activated persulfate. Chemosphere 86(11), 1092-1097.

Betterton, E.A., Hoffmann, M.R., 1990. Kinetics and mechanism of the oxidation of aqueous hydrogen sulfide by peroxymonosulfate. Environ. Sci. Technol. 24(12), 1819-1824.

Bolton, J.R., Bircher, K.G., Tumas, W., Tolman, C.A., 2001. Figures-of-merit for the technical development and application of advanced oxidation technologies for both electric- and solar-driven systems (IUPAC Technical Report). Pure Appl. Chem. 73(4), 627-637.

Buxton, G.V., Greenstock, C.L., Helman, W.P., Ross, A.B., 1988. Critical review of rate constants for reactions of hydrated electrons, hydrogen atoms and hydroxyl radicals ($\cdot OH/\cdot O^-$) in Aqueous Solution. J. Phys. Chem. Ref. Data 17(2), 513-886.

Chen, S., Xiong, P., Zhan, W., Xiong, L., 2018. Degradation of ethylthionocarbamate by pyrite-activated persulfate. Miner. Eng. 122, 38-43.

Cheng, H., Lin, H., Huo, H., Dong, Y., Xue, Q., Cao, L., 2012. Continuous removal of ore floatation reagents by an anaerobic–aerobic biological filter. Bioresour.

Technol. 114, 255-261.

Deng, J., Shao, Y., Gao, N., Xia, S., Tan, C., Zhou, S., Hu, X., 2013. Degradation of the antiepileptic drug carbamazepine upon different UV-based advanced oxidation processes in water. Chem. Eng. J. 222, 150-158.

Devi, P., Das, U., Dalai, A.K., 2016. In-situ chemical oxidation: Principle and applications of peroxide and persulfate treatments in wastewater systems. Sci. Total Environ. 571, 643-657.

Dold, B., 2017. Acid rock drainage prediction: A critical review. J. Geochem. Explor. 172, 120-132.

Flanagan, J., Griffith, W.P., Skapski, A.C., 1984. The active principle of Caro's acid, HSO_5^-: X-ray crystal structure of $KHSO_5 \cdot H_2O$. J. Chem. Soc., Chem. Commun. 0(23), 1574-1575.

Fu, P., Feng, J., Yang, T., Yang, H., 2015. Comparison of alkyl xanthates degradation in aqueous solution by the O_3 and UV/O_3 processes: Efficiency, mineralization and ozone utilization. Miner. Eng. 81, 128-134.

Ghanbari, F., Moradi, M., Gohari, F., 2016. Degradation of 2,4,6-trichlorophenol in aqueous solutions using peroxymonosulfate/activated carbon/UV process via sulfate and hydroxyl radicals. J. Water Process. Eng. 9, 22-28.

Guan, Y., Ma, J., Li, X., Fang, J., Chen, L., 2011. Influence of pH on the formation of sulfate and hydroxyl radicals in the UV/peroxymonosulfate system. Environ. Sci. Technol. 45(21), 9308-9314.

Guo, Y., Cui, K., Hu, M., Jin, S., 2017. Fe(III) ions enhanced catalytic properties of $(BiO)_2CO_3$ nanowires and mechanism study for complete degradation of xanthate. Chemosphere 181, 190-196.

Hu, Y., Wang, D., Xu, Z., 1997. A study of interactions and flotation of wolframite with octyl hydroxamate. Miner. Eng. 10(6), 623-633.

Khan, J.A., He, X., Shah, N.S., Khan, H.M., Hapeshi, E., Fatta-Kassinos, D., Dionysiou, D.D., 2014. Kinetic and mechanism investigation on the photochemical degradation of atrazine with activated H_2O_2, $S_2O_8^{2-}$ and HSO_5^-. Chem. Eng. J. 252, 393-403.

Kwon, M., Kim, S., Yoon, Y., Jung, Y., Hwang, T.-M., Lee, J., Kang, J.-W., 2015. Comparative evaluation of ibuprofen removal by UV/H_2O_2 and UV/$S_2O_8^{2-}$ processes for wastewater treatment. Chem. Eng. J. 269, 379-390.

Lente, G., Kalmár, J., Baranyai, Z., Kun, A., Kék, I., Bajusz, D., Takács, M., Veres, L., Fábián, I., 2009. One- versus two-electron oxidation with peroxomonosulfate ion: Reactions with iron(II), vanadium(IV), halide ions, and photoreaction with cerium(III). Inorg. Chem. 48(4), 1763-1773.

Mahmoud, M.E., Osman, M.M., Hafez, O.F., Elmelegy, E., 2010. Removal and preconcentration of lead(II), copper(II), chromium(III) and iron(III) from wastewaters by surface developed alumina adsorbents with immobilized 1-nitroso-2-naphthol. J. Hazard. Mater. 173(1), 349-357.

Mark, G., Schuchmann, M.N., Schuchmann, H.-P., Von Sonntag, C., 1990. The

photolysis of potassium peroxodisulphate in aqueous solution in the presence of tert-butanol: a simple actinometer for 254 nm radiation. J. Photochem. Photobiol. A: Chem. 55(2), 157-168.

Molina, G.C., Cayo, C.H., Rodrigues, M.a.S., Bernardes, A.M., 2013. Sodium isopropyl xanthate degradation by advanced oxidation processes. Miner. Eng. 45, 88-93.

Muruganandham, M., Swaminathan, M., 2004. Photochemical oxidation of reactive azo dye with UV-H_2O_2 process. Dye. Pigment. 62, 269–275.

Neyens, E., Baeyens, J., 2003. A review of classic Fenton's peroxidation as an advanced oxidation technique. J. Hazard. Mater. 98(1), 33-50.

Parsons, S. 2004. Advanced oxidation processes for water and wastewater treatment. IWA publishing. London.

Piechowski, M.V., Thelen, M.-A., Hoigné, J., Bühler, R.E., 1992. *tert*-butanol as an OH-scavenger in the pulse radiolysis of oxygenated aqueous systems. Ber. Bunsenges. Phys. Chem. 96(10), 1448-1454.

Pozdnyakova, N.N., Nikiforova, S.V., Turkovskaya, O.V., 2010. Influence of PAHs on ligninolytic enzymes of the fungus Pleurotus ostreatus D1. Cent. Eur. J. Biol. 5(1), 83-94.

Pubchem. 2019. Compound summary for CID 8580. pubchem.ncbi.nlm.nih.gov/compound/1-Nitroso-2-naphthol#section=GHS-Classification. (accessed 13 June 2019).

Rehman, F., Sayed, M., Khan, J.A., Shah, N.S., Khan, H.M., Dionysiou, D.D., 2018. Oxidative removal of brilliant green by UV/$S_2O_8^{2-}$, UV/HSO_5^- and UV/H_2O_2 processes in aqueous media: A comparative study. J. Hazard. Mater. 357, 506–514.

Rezaei, R., Massinaei, M., Zeraatkar Moghaddam, A., 2018. Removal of the residual xanthate from flotation plant tailings using modified bentonite. Miner. Eng. 119, 1-10.

Shah, N.S., He, X., Khan, H.M., Khan, J.A., O'shea, K.E., Boccelli, D.L., Dionysiou, D.D., 2013. Efficient removal of endosulfan from aqueous solution by UV-C/peroxides: A comparative study. J. Hazard. Mater. 263, 584-592.

Sharma, J., Mishra, I.M., Kumar, V., 2015. Degradation and mineralization of bisphenol A (BPA) in aqueous solution using advanced oxidation processes: UV/H_2O_2 and UV/$S_2O_8^{2-}$ oxidation systems. J. Environ. Manage. 156, 266-275.

Spiliotopoulou, A., Hansen, K.M.S., Andersen, H.R., 2015. Secondary formation of disinfection by-products by UV treatment of swimming pool water. Sci. Total Environ. 520, 96-105.

Tan, C., Gao, N., Deng, Y., An, N., Deng, J., 2012. Heat-activated persulfate oxidation of diuron in water. Chem. Eng. J. 203, 294-300.

Weber, J., Kurková, R., Klánová, J., Klán, P., Halsall, C.J., 2009. Photolytic degradation of methyl-parathion and fenitrothion in ice and water: Implications for cold environments. Environ. Pollut. 157(12), 3308-3313.

Wei, H., Gao, B., Ren, J., Li, A., Yang, H., 2018. Coagulation/flocculation in dewatering of sludge:A review. Water Res. 143, 608–631.

Xie, P., Ma, J., Liu, W., Zou, J., Yue, S., Li, X., Wiesner, M.R., Fang, J., 2015. Removal of 2-MIB and geosmin using UV/persulfate: Contributions of hydroxyl and sulfate radicals. Water Res. 69, 223-233.

Yan, P., Chen, G., Ye, M., Sun, S., Ma, H., Lin, W., 2016. Oxidation of potassium n-butyl xanthate with ozone: Products and pathways. J. Clean. Prod. 139, 287-294.

Yang, S., Wang, P., Yang, X., Shan, L., Zhang, W., Shao, X., Niu, R., 2010. Degradation efficiencies of azo dye Acid Orange 7 by the interaction of heat, UV and anions with common oxidants: Persulfate, peroxymonosulfate and hydrogen peroxide. J. Hazard. Mater. 179(1), 552-558.

Yao, H., Sun, P., Minakata, D., Crittenden, J.C., Huang, C., 2013. Kinetics and modeling of degradation of ionophore antibiotics by UV and UV/H_2O_2. Environ. Sci. Technol. 47(9), 4581-4589.

Zhang, W., Gao, Y., Qin, Y., Wang, M., Wu, J., Li, G., An, T., 2019. Photochemical degradation kinetics and mechanism of short-chain chlorinated paraffins in aqueous solution: A case of 1-chlorodecane. Environ. Pollut. 247, 362-370.

Zhou, L., Song, W., Chen, Z., Yin, G., 2013. Degradation of organic pollutants in wastewater by bicarbonate-activated hydrogen peroxide with a supported cobalt catalyst. Environ. Sci. Technol. 47(8), 3833-3839.

Zhu, X., Yao, J., Wang, F., Yuan, Z., Liu, J., Jordan, G., Knudsen, T.Š., Avdalović, J., 2018. Combined effects of antimony and sodium diethyldithiocarbamate on soil microbial activity and speciation change of heavy metals. Implications for contaminated lands hazardous material pollution in nonferrous metal mining areas. J. Hazard. Mater. 349, 160-167.

Figure Captions

Fig. 1. Comparison of different systems for αNβN degradation. Inset: Comparison of pseudo-first-order dynamics constant *k* of αNβN decay in different oxidation systems. UVA/B-based advanced oxidation processes (a); **oxidant alone (b).** Experimental conditions: [αNβN] = 0.1 mM; [HP] = [SPS] = [PMS] = 10 mM; no pH adjustment (Initial pH = 6.3, $pH_{0,[HP]}$ = 5.3, $pH_{0,[SPS]}$ = 3.7, $pH_{0,[PMS]}$ = 2.4); UVA-B power = 500 W; temperature = 25 ± 1°C.

Fig. 2. Effect of oxidant concentration on degradation of αNβN by UVA-B-activated systems. Experimental conditions: [αNβN] = 0.1 mM; pH = 6.0; UVA-B power = 500 W; temperature = 25 ± 1 °C.

Fig. 3. Effect of UVA-B power on degradation of αNβN by UVA-B-activated systems. Experimental conditions: [αNβN] = 0.1 mM, [HP] = [PMS] = 50 mM, [SPS] = 10 mM; pH = 6.0; temperature = 25 ± 1 °C.

Fig. 4. Effect of NO_3^-, SO_4^{2-}, Cl^- and HCO_3^- on degradation of αNβN by UVA-B-activated systems. Experimental conditions: [αNβN] = 0.1 mM, [HP] = [SPS] = [PMS] = 10 mM; pH = 6.0; UVA-B power = 500 W; temperature = 25 ± 1°C.

Fig. 5. Effect of free radical inhibitors on degradation of αNβN by UVA-B/HP (a), UVA-B/SPS (b), and UVA-B/PMS (c) systems. Comparison of

pseudo-first-order dynamics constant *k* of αNβN decay in different oxidation systems (d). Experimental conditions: [αNβN] = 0.1 mM, [HP] = [SPS] = [PMS] = 10 mM; no pH adjustment (Initial pH = 6.3, $pH_{0,[HP]}$ = 5.3, $pH_{0,[SPS]}$ = 3.7, $pH_{0,[PMS]}$ = 2.4); UVA-B power = 500 W; temperature = 25 ± 1 °C.

List of Tables

Table 1. Effect of pH on degradation of αNβN by UVA-B-activated oxidants.

Experimental conditions: [**αNβN**] = 0.1 mM, [HP] = [SPS] = [PMS] = 10 mM;

UVA-B power = 500 W; temperature = 25 ± 1 °C.

System	Initial pH	$pH_{0,oxidant}$	Final pH	$k/10^{-2}$ (min^{-1})	R^2
UVA-B	6.3	6.3	6.3	\	\
UVA-B/HP	6.3	5.5	4.6	0.63 ± 0.03	0.9996
	2.0	2.0	2.0	0.54 ± 0.08	0.9987
	4.0	4.0	4.0	0.64 ± 0.1	0.9976
	6.0	5.8	5.1	0.62 ± 0.1	0.9980
UVA-B/SPS	6.3	3.9	3.2	3.1 ± 0.1	0.9986
	2.0	1.9	1.9	3.2 ± 0.2	0.9931
	8.0	4.0	2.9	3.0 ± 0.6	0.9811
	9.0	6.2	3.4	3.2 ± 0.2	0.9910
UVA-B/PMS	6.3	2.3	2.3	0.61 ± 0.02	0.9977
	4.0	2.3	2.3	0.58 ± 0.08	0.9983
	11.8	6.3	2.4	0.64 ± 0.1	0.9940
	11.9	7.4	3.4	0.56 ± 0.03	0.9912

Table 2. Comparison of UVA-B-activated oxidants in αNβN degradation with respect to the energy requirements and oxidant costs. Experimental conditions: [αNβN] = 0.1 mM; [HP] = [SPS] = [PMS] = 10 mM; no pH adjustment (Initial pH = 6.3, $pH_{0,[HP]}$ = 5.3, $pH_{0,[SPS]}$ = 3.7, $pH_{0,[PMS]}$ = 2.4); UVA-B power = 500 W; temperature = 25 ± 1 □.

system	$E_{EO}/10^5$ (kWh m^{-3})	Oxidants costs/10^{-2} (dollars g^{-1})[a]
UVA-B	\	\
UVA-B/HP	1.2	1.3
UVA-B/SPS	0.24	0.74
UVA-B/PMS	1.2	18

[a] The price of oxidants was supplied by Sinopharm Chemical Reagent Co. Ltd. (Shanghai, China) in 2019.

Table 3. The identified αNβN and its possible intermediates products during the UVA-B/oxidant processes.

Products	Retention time (min)	Chemical Names	Molecular Formula	CAS No.	Proposed Structure	UV/HP	UV/SPS	UV/PMS
αNβN	17.94	α-Nitroso-β-naphthol	$C_{10}H_7NO$	171-91-9	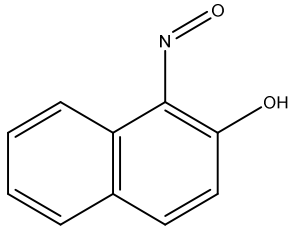	√	√	√
1	11.80	2-Cyanobenzaldehyde	C_8H_5NO	7468-67-9	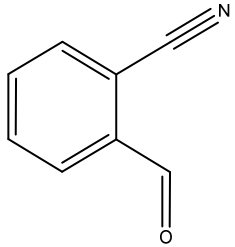	√	√	√
2	12.16	1,2-Benzenedicarboxaldehyde	$C_8H_6O_2$	643-79-8	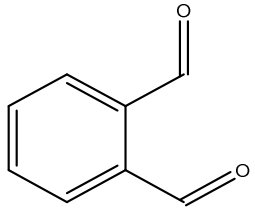	×	√	×

3	13.13	1,2-Benzenedicarboxylic acid	$C_8H_6O_4$	88-99-3	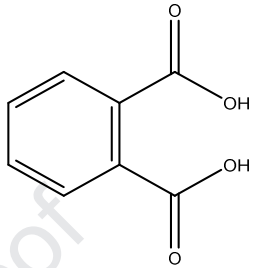	√	√	√
4	13.13	Phthalic anhydride	$C_8H_4O_3$	85-44-9	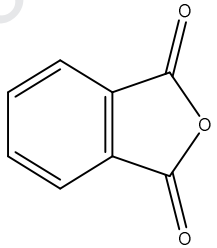	√	√	√
5	13.63	1(3H)-Isobenzofuranone	$C_8H_6O_2$	87-41-2	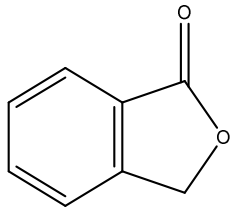	√	√	√
6	14.41	Coumarin	$C_9H_6O_2$	91-64-5	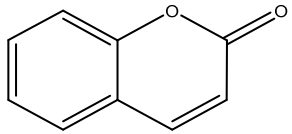	√	√	√

7	14.41	o-Hydroxy-trans-cinnamic acid	$C_9H_6O_3$	614-60-8	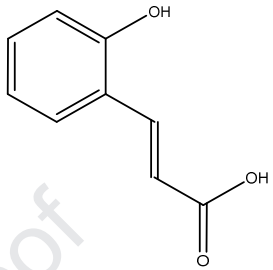	√	√	√
8	15.21	o-Cyanobenzoic acid	$C_8H_5NO_2$	3839-22-3	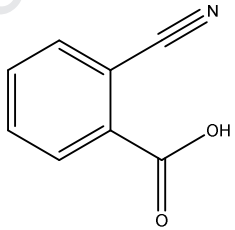	√	√	√
9	15.92	β-Naphthol	$C_{10}H_8O$	135-19-3	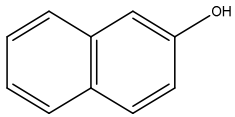	√	√	√
10	18.62	α-Nitro-β-naphthol	$C_{10}H_7NO_3$	550-60-7	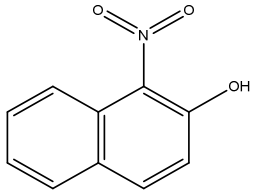	√	√	√

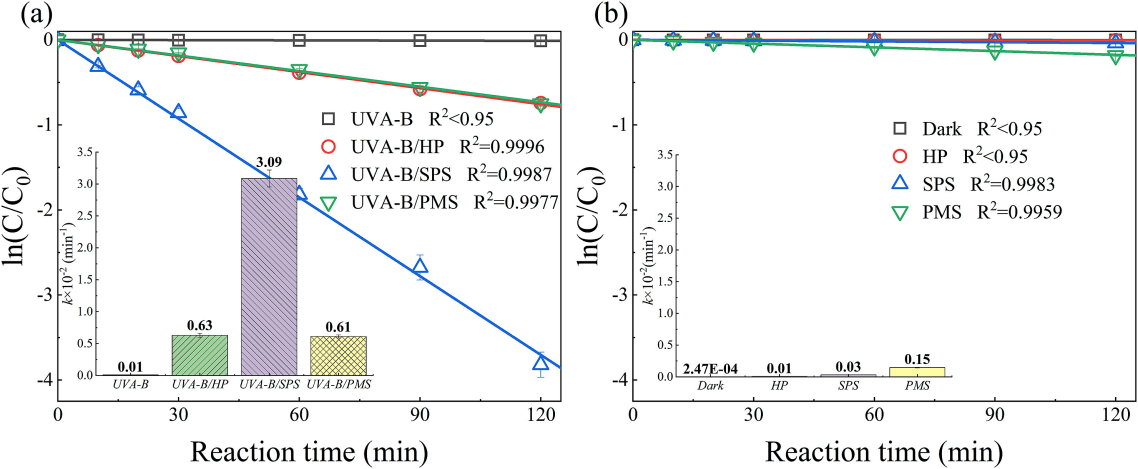
(a)
UVA-B R^2<0.95
UVA-B/HP R^2=0.9996
UVA-B/SPS R^2=0.9987
UVA-B/PMS R^2=0.9977
ln(C/C0)
Reaction time (min)
k×10-2 (min-1)
0.01
0.63
3.09
0.61
UVA-B
UVA-B/HP
UVA-B/SPS
UVA-B/PMS
(b)
Dark R^2<0.95
HP R^2<0.95
SPS R^2=0.9983
PMS R^2=0.9959
ln(C/C0)
Reaction time (min)
k×10-2 (min-1)
2.47E-04
0.01
0.03
0.15
Dark
HP
SPS
PMS

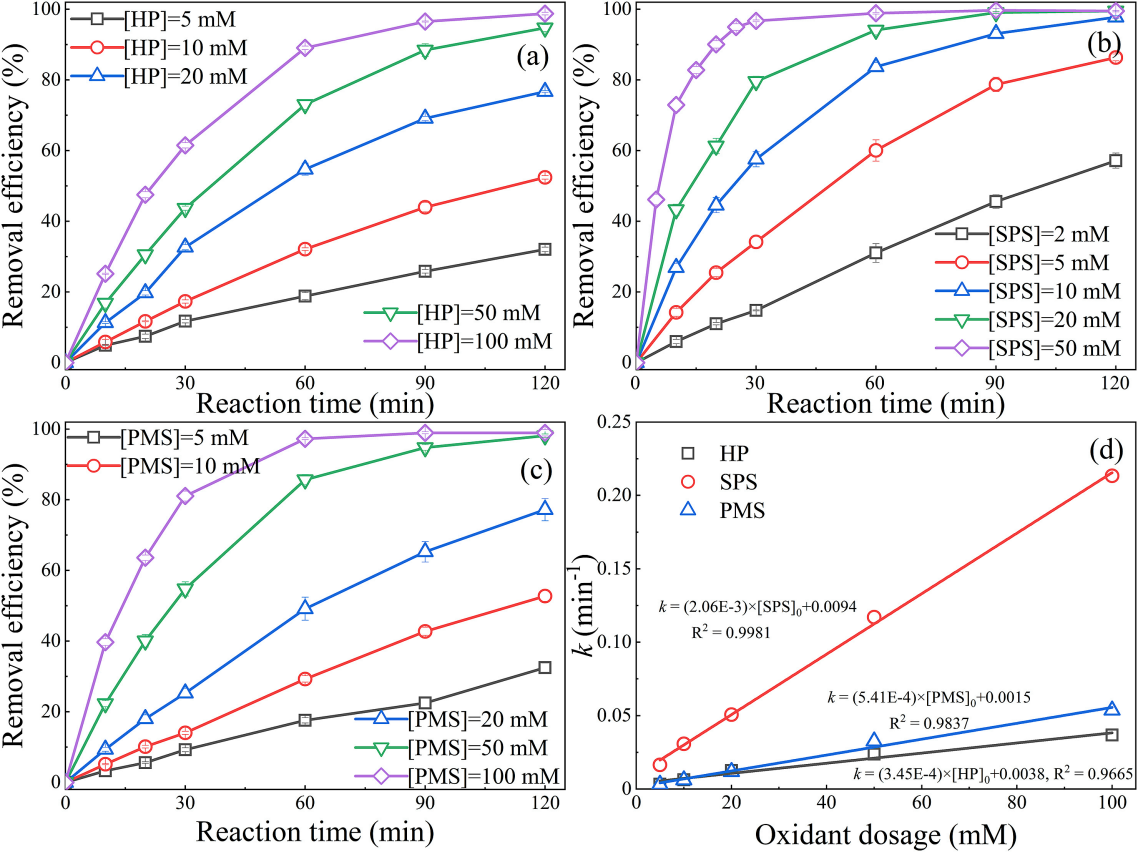
(a)
[HP]=5 mM
[HP]=10 mM
[HP]=20 mM
[HP]=50 mM
[HP]=100 mM
Removal efficiency (%)
Reaction time (min)
(b)
[SPS]=2 mM
[SPS]=5 mM
[SPS]=10 mM
[SPS]=20 mM
[SPS]=50 mM
Removal efficiency (%)
Reaction time (min)
(c)
[PMS]=5 mM
[PMS]=10 mM
[PMS]=20 mM
[PMS]=50 mM
[PMS]=100 mM
Removal efficiency (%)
Reaction time (min)
(d)
HP
SPS
PMS
k = (2.06E-3)×[SPS]0+0.0094
R2 = 0.9981
k = (5.41E-4)×[PMS]0+0.0015
R2 = 0.9837
k = (3.45E-4)×[HP]0+0.0038, R2 = 0.9665
k (min-1)
Oxidant dosage (mM)

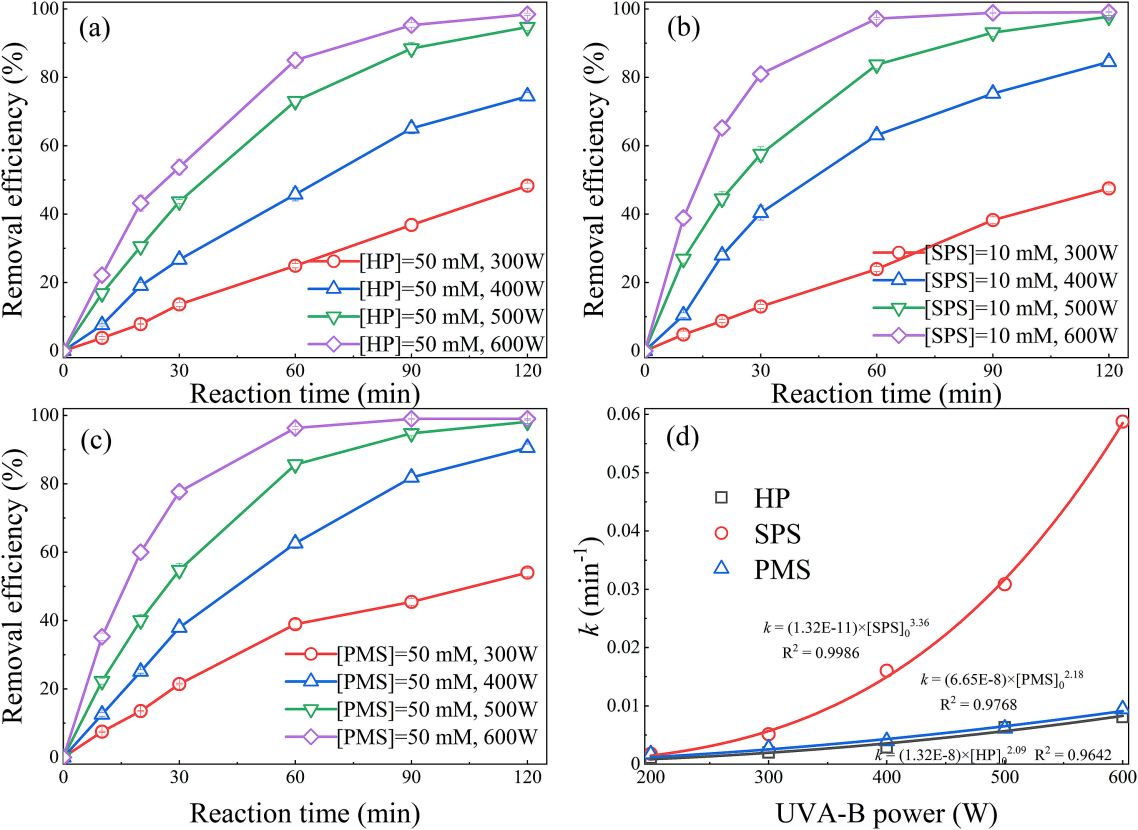
(a)
Removal efficiency (%)
Reaction time (min)
[HP]=50 mM, 300W
[HP]=50 mM, 400W
[HP]=50 mM, 500W
[HP]=50 mM, 600W
(b)
Removal efficiency (%)
Reaction time (min)
[SPS]=10 mM, 300W
[SPS]=10 mM, 400W
[SPS]=10 mM, 500W
[SPS]=10 mM, 600W
(c)
Removal efficiency (%)
Reaction time (min)
[PMS]=50 mM, 300W
[PMS]=50 mM, 400W
[PMS]=50 mM, 500W
[PMS]=50 mM, 600W
(d)
HP
SPS
PMS
k (min-1)
UVA-B power (W)
k = (1.32E-11)×[SPS]0 3.36
R2 = 0.9986
k = (6.65E-8)×[PMS]0 2.18
R2 = 0.9768
k = (1.32E-8)×[HP]0 2.09 R2 = 0.9642

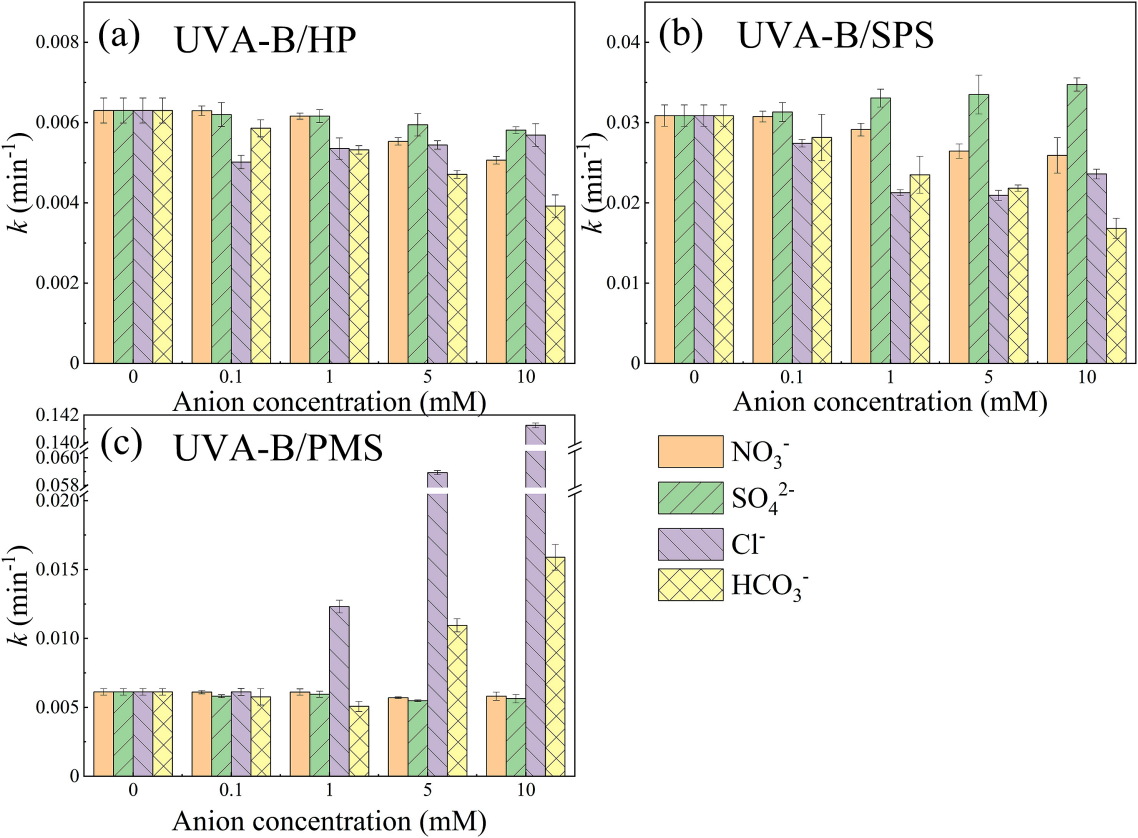
(a)
UVA-B/HP
k (min-1)
0.008
0.006
0.004
0.002
0
0
0.1
1
5
10
Anion concentration (mM)
(b)
UVA-B/SPS
k (min-1)
0.04
0.03
0.02
0.01
0
0
0.1
1
5
10
Anion concentration (mM)
(c)
UVA-B/PMS
k (min-1)
0.142
0.140
0.060
0.058
0.020
0.015
0.010
0.005
0
0
0.1
1
5
10
Anion concentration (mM)
NO3-
SO42-
Cl-
HCO3-

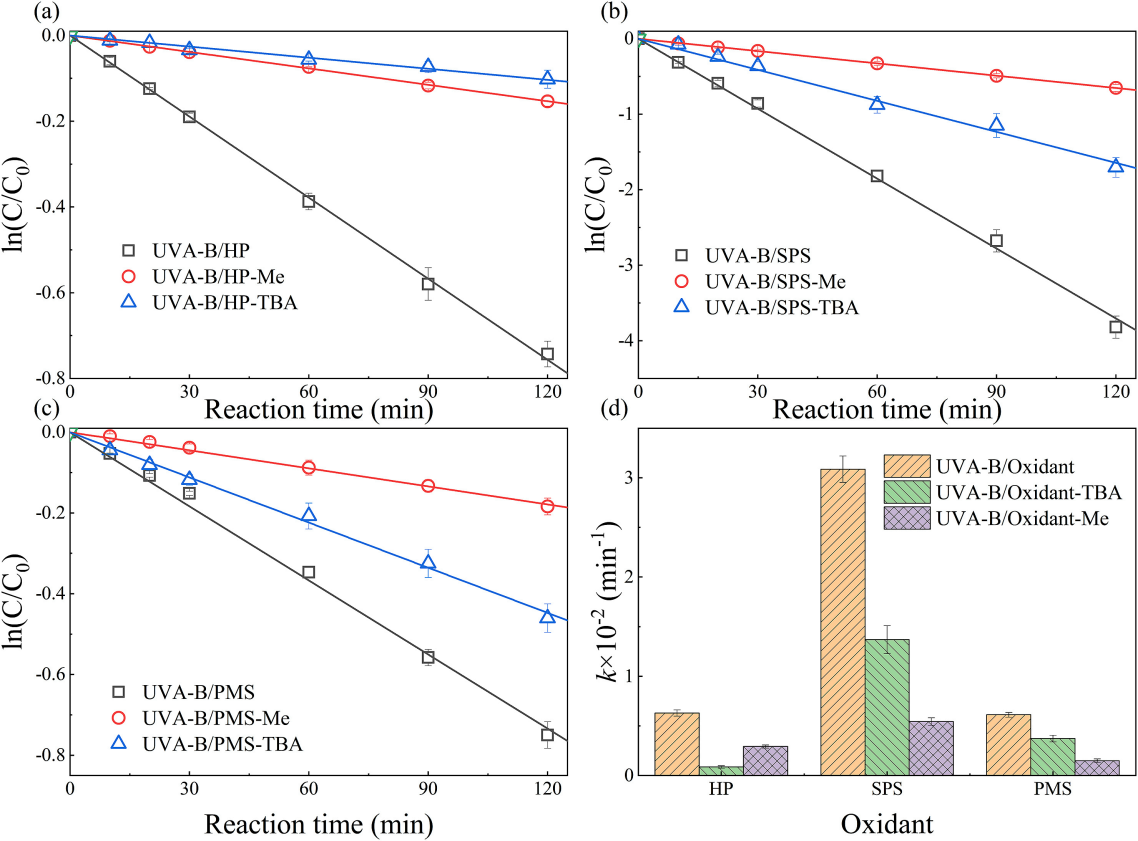
(a)
ln(C/C0)
Reaction time (min)
UVA-B/HP
UVA-B/HP-Me
UVA-B/HP-TBA
(b)
ln(C/C0)
Reaction time (min)
UVA-B/SPS
UVA-B/SPS-Me
UVA-B/SPS-TBA
(c)
ln(C/C0)
Reaction time (min)
UVA-B/PMS
UVA-B/PMS-Me
UVA-B/PMS-TBA
(d)
k×10-2 (min-1)
Oxidant
HP
SPS
PMS
UVA-B/Oxidant
UVA-B/Oxidant-TBA
UVA-B/Oxidant-Me

Highlights

- Degradation of α-nitroso-β-naphthol was made in UVA-B/HP, UVA-B/SPS and UVA-B/PMS systems.
- UVA-B/SPS was found to be the most efficient, economical and energy-saving.
- High concentration of Cl^- enhances the degradation of αNβN in UVA-B/PMS systems.
- 10 by-products from the degradation of αNβN in three UVA-B/oxidant systems were detected.